Low Cost PM Synchronous Servo-Applications Employing Asynchronous-Motor Frame

Claudio Bianchini[1], Matteo Davoli[1], Gianmario Pellegrino[2], Fabio Immovilli[1], Emilio Lorenzani[1]

[1] DISMI - University of Modena and Reggio Emilia, Italy
[2] DEE - Politecnico di Torino, Italy

Abstract—**This paper presents a comparison among low cost permanent magnet synchronous machine (PMSM) solutions, employing the frame and the stator laminations of an asynchronous machine. The comparison is carried out by means of finite element simulations. This work aims at obtaining machines with reduced cost, competitive in terms of nominal torque, torque ripple and cogging torque.**

The baseline for comparison is a surface mounted PMSM with high-strength magnets and non-skewed rotor. In order to reduce torque ripple and cogging torque, magnets with sinusoidal profiles radial wise are first introduced. Second, enhanced hybrid permanent magnets poles are adopted, replacing part of high strength NdFeB material with cheaper ferrite to reduce the production costs of the magnetic pole. Finally these PMSMs are compared to a synchronous reluctance and ferrite-assisted synchronous reluctance machines.

The presented results indicate that the hybrid-magnets solution is the best trade-off between performance, cost and manufacturability and that the ferrite-assisted synchronous reluctance machine is quite competitive and low cost.

Index Terms—**Brushless machines, cogging torque, ferrite, PM assisted synchronous reluctance machine, magnet cost, modular pole, sinusoidally profiled magnets, torque ripple.**

I. INTRODUCTION

The asynchronous machine is the most widespread electric motor due to its affordability, ruggedness and good performance. Nevertheless, the increasing demand for high efficiency motors, dictated by the new efficiency classes IE3 and IE4 [1], [2], has renewed the interest in substituting asynchronous motors with permanent magnet synchronous machine (PMSM) or synchronous reluctance machine. PMSM are characterized by higher torque density, higher efficiency (no rotor Joule losses and no magnetizing current), high dynamic performance (moreover it is possible to employ high number of poles to further increase torque density). With respect to the asynchronous machine, they present also some disadvantages such as: cogging torque, torque ripple under load, demagnetization risk especially when the magnet are exposed directly to air-gap flux and the high cost of rare-earth permanent magnets (PM). Indeed, the cost of rare-earth PM materials (e.g. NdFeB) constitutes a significant fraction of a PM machine manufacture costs. Many manufacturers would be glad to offer the super-premium efficiency PMSM solution within the same frame and stator stack of their current stock of induction motors, provided that the PM cost and other side effects are minimized.

This paper deals with possible cost reduction of PMSM motors, with different PM rotors designed for the same induction motor stator. A modular pole configuration was proposed in [3], where high strength NdFeB PMs are alternated to NdFeB PMs of lower remanence, in order to mimic a sinusoidal magneto motive force (MMF) distribution at the air-gap. However the increased complexity resulted in a higher overall production cost. Therefore, this idea has been abandoned. Alternatively, the strong NdFeB can be flanked by cheap ferrite magnets leading to a better tradeoff between performance and cost. This is the basic construction of the hybrid magnet rotor proposed in [4], used also in this comparison. A surface mounted PM rotor with the PM poles rounded, will be considered in this paper to minimize torque ripple and cogging torque without skewing. Synchronous reluctance and ferrite assisted synchronous reluctance will be also evaluated. These solutions strongly reduce the rotor cost thanks to maximized reluctance torque and use of ferrite magnets.

The optimization of PMSMs must take into account the reduction of torque ripple and cogging torque, considered key indicators of the motor performance quality. Load torque ripple results from the interaction between the high harmonics of air-gap magnetic field produced by stator winding and the magnetic field harmonics produced by the rotor permanent magnets. In order to minimize this unwanted effect there are some strategies that can be employed:
- the reduction of the harmonic content of the air-gap flux density distribution, exploited in this paper by the sinusoidally rounded magnets rotor;
- harmonic cancellation techniques such as the rotor or stator skewing or the rotor step skewing;
- avoid stator and rotor harmonic interaction choosing appropriate number of stator slot and rotor flux barriers [5] or hybrid magnet rotor step [4].

Since load torque ripple arises from interaction between stator current and rotor MMF while the cogging torque depends by the interaction between rotor magnet and stator slot openings. Therefore some of the aforementioned techniques for load torque ripple reduction could be negatively affect the cogging torque.

Laminated rotor construction is mandatory for synchronous reluctance machines and could be beneficial also for surface PM machines, because in addition to reducing the iron rotor

6090

losses, it can incorporate the magnet seating notches, thus avoiding the requirements for a fixture during magnets gluing phase. This is also a rational choice from the manufacturing point of view, as the rotor could be obtained from the scrap of the stator punching process. Under these assumptions the cost analysis of the machine could be brought back to the cost of the permanent magnet component employed in the different rotor solutions (Tab. IV).

A traditional induction motor (IM) stator with 36 slots and 6 poles was chosen as the reference stator for this paper. The different rotor solutions were compared in terms of nominal achievable torque, load torque ripple, cogging torque, power factor and magnet volume. The reference PM machine is presented in section II, in section III a rounded magnet rotor solution is presented, the machine with hybrid magnet is presented in section IV, the synchronous reluctance rotors are presented in section V and VI, and finally in section VII the comparison of the different rotor solution were compared.

II. REFERENCE MACHINE

In the reference machine, the squirrel cage rotor of the IM was substituted with a six-pole PMSM rotor with the PM cylindrical profile represented in Fig. 1. The main ratings of this machine are reported in Tab. I and they are used as base value for the different rotor designs proposed in this paper. The results of the comparison are summarized in Tab. III.
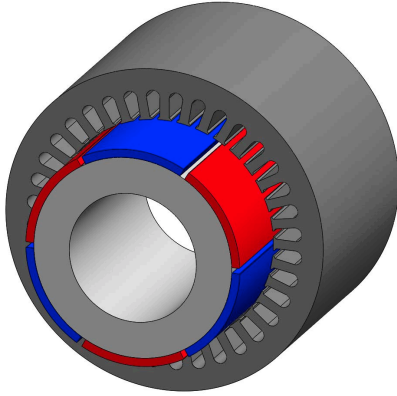

Fig. 1. 36-6 Reference Machine

TABLE I
REFERENCE MACHINE RATING PLATE

Slots-Poles Number	36-6	-
Stator External Diameter	175	mm
Axial Length	110	mm
PM thickness	4.5	mm
Slot Conductors	20	-
Nominal speed	1000	rpm
Nominal Current Density	4.5	A/mm^2
Overload Current Density	9.0	A/mm^2
Filling Factor	0.432	-

Despite the large number of slots per-pole per-phase produces a low harmonic content of the magneto-motive force in the air-gap, the reference machine shows a significant torque ripple and cogging torque, due to: high harmonic content of rotor MMF; stator saturation emphasized by the tooth design of induction motors laminations and the integer slot-pole ratio. The use of simple magnets with uniform thickness thus becomes inadvisable.

III. ROTOR WITH SINUSOIDALLY ROUNDED MAGNETS

A first alternative to reduce the disadvantages described in the previous section, is the use of rounded magnets (Fig. 2).
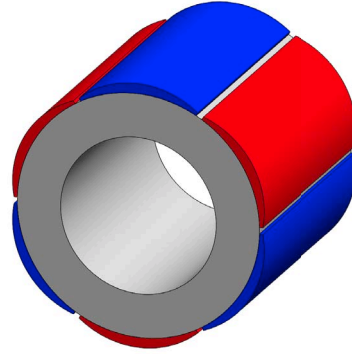

Fig. 2. Rotor with Sinusoidally Rounded Magnets

By estimating air-gap flux density as a function of the permanent magnet thickness and equating it to a sinusoid (Eq. 1), it is possible to find the magnet profile that produces the ideal air-gap flux density distribution (Eq. 2).

$$B_m = \frac{B_{r,m}}{1 + \mu_{r,m}(\frac{g}{l_m} - 1)} = B_g \cdot \sin(\theta_e) \tag{1}$$

$$l_m = \frac{g}{\frac{(\frac{B_{r,m}}{B_g \cdot \sin(\theta_e)} - 1)}{\mu_{r,m}} + 1} \tag{2}$$

Where B_m is the magnet working point, $B_{r,m}$ is magnet remanence, $\mu_{r,m}$ is magnet relative permeability, l_m is the magnet thickness, B_g is the ideal air-gap flux density and θ_e is the electrical angle. To ensure a good magnetization of the material and avoid brittleness, it is required to maintain a minimum thickness along the sides of the magnets, as shown in (Fig. 2). The resulting air gap flux density distribution is shown in Fig. 3. In this way the harmonic content of the flux density produced by the rotor along the air-gap is small (Fig. 4) and therefore load torque ripple and cogging torque are strongly reduced. Moreover, sinusoidal flux linkage and back-electromotive force are obtained. The minor harmonic content of magneto-motive force together with the greater air-gap reduce the magnetic saturation at the teeth and the pole pieces of the stator.

IV. HYBRID MAGNETS WITH INTERNAL POLE SKEWING ROTOR

The hybrid magnet design named internal skewing pole proposed in [4] is here evaluated using the same stator of the reference machine. The pole is constructed by surrounding the
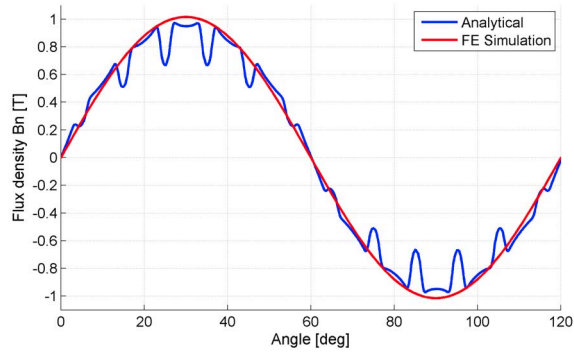
Fig. 3. Air-Gap Flux Density Distribution Using Rounded Magnets Rotor
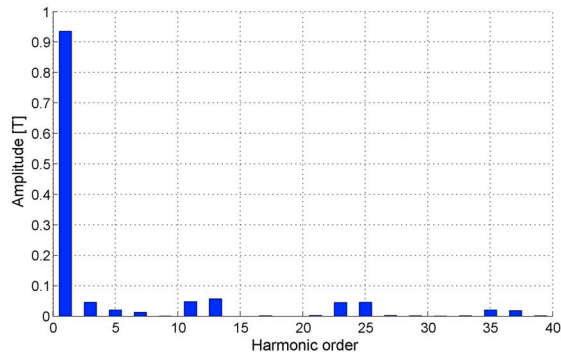

Fig. 4. Air-Gap Flux Density Distribution FFT Using Rounded Magnets Rotor

rare earth NdFeB PM placed in the center of the pole with a ferrite PM (Fig. 5).
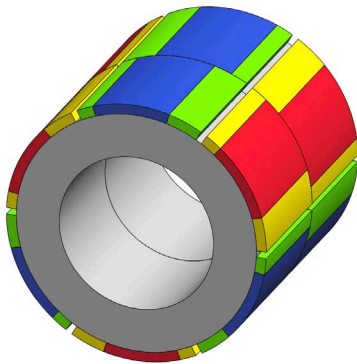

Fig. 5. Hybrid Internal Pole Skewing Rotor With Rare Earth NdFeB (red and blue) and Ferrite (yellow and green) PM.

The aim is to discretize the ideal sinusoidal air-gap flux density as the sum of the contributions of the rotor steps. To obtain this, the same algorithm developed in [4] is here employed to determinate the correct arc angle of the different magnets obtaining the discretization shown in Fig. 6, where the highest level of flux density corresponds to two steps of NdFeB, the lowest level to two step of ferrite and the intermediate level correspond to the average of the remanence

of the two different magnets. In this case, thanks to the high number of the stator slots per pole, it is possible to reduce the number of the axial rotor step at only two. For this reason, the disctretization of the ideal sinusoidal flux density distribution result quite poor, but in this application the resulting torque ripple is anyway acceptable. The assembly is consequently simplified, implying a reduction in the manufacturing cost.
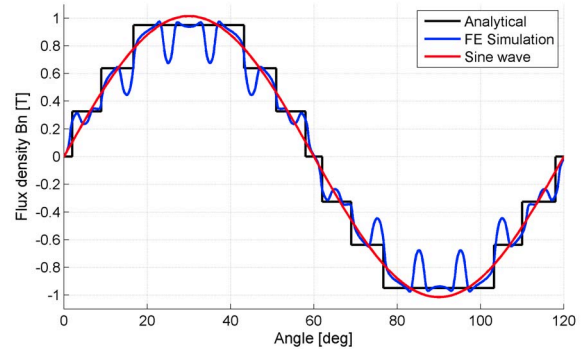

Fig. 6. Three-Dimensional Discretization of the Ideal Sinusoidal Flux Density Distribution Using 2-step Hybrid Rotor
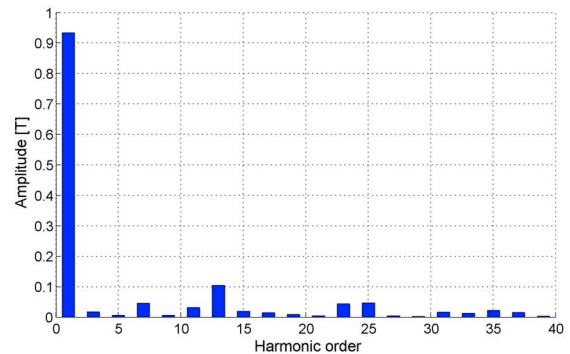

Fig. 7. Air-Gap Flux Density Distribution FFT using 2-step Hybrid Rotor

Using FE simulations the three dimensional resulting flux density distribution was evaluated Fig. 6, where it is also shown the effect of the slot openings.

Comparing the FFT of the air-gap flux density distribution of the hybrid rotor (Fig. 7) with that of the rounded magnets (Fig. 4). The little additional harmonic contributions introduced by the hybrid solution, is worth noticing in particular relating to the slot-harmonics.

It should be noted that using only two steps at rotor, the two half-rotors are exactly the same. Therefore it is possible to manufacture a single type of half-rotor and assemble two of this in the opposite manner, thus further reducing production costs.

When employing ferrite magnets, the admissible maximum current in overload is limited in order to avoid partial demagnetization. In this case, maximum current results limited at two time the nominal current. Actually this aspect isn't a real problem for customers of this kind of low cost motors, because their applications don't request higher overload ability.

6092

V. SYNCHRONOUS RELUCTANCE ROTOR

Another possible design solution to reduce manufacturing costs of the machine and increasing the efficiency of the base IM is the synchronous reluctance topology [6]. In this case the original squirrel cage rotor is substituted with a laminated rotor (Fig. 8) using an appropriate number of layers in order to reduce torque ripple [5]. The rotor design was optimized using *Syre* algorithm [7].

Fig. 8. Reluctance Rotor

In this case the absence of the magnet leads to a solution with zero cogging torque and, moreover, no problem of demagnetization could arise from overload current or high temperature. The main drawbacks of this topology are the lower load performance and the intrinsic poor power factor of the machine that requires an higher volt-ampere rating of the drive.

VI. FERRITE ASSISTED RELUCTANCE ROTOR

In order to improve the disadvantages mentioned in the previous section a ferrite assisted reluctance motor (Fig. 9) was also added to this comparison to achieve a more in-depth exploration of possible solutions. The costs increasing due to the use of ferrite PM is justified by a significant improvement in load performance and power factor. Cogging torque results slightly higher compared to the sinusoidally rounded solution.

The presence of internal permanent magnet makes this solution less prone to demagnetization compared to surface permanent magnet topology.

As for the previous solution it must be highlighted that this kind of machine is capable of flux weakening operation and therefore the possible application fields benefits of the resulting increased speed range.

VII. RESULTS COMPARISON

The resulting waveform of the electromotive force of one phase at 1000 rpm is reported in Fig. 10, while the cogging torque is shown in Fig. 11. Torque and torque ripple at 4.5 and 9 A/mm2 are shown in figure Fig. 12 and Fig. 13. The maximum flux density of the stator in the different machines at nominal load are reported in Tab. II. The numerical results of the simulated performance are summarized in Tab. III.
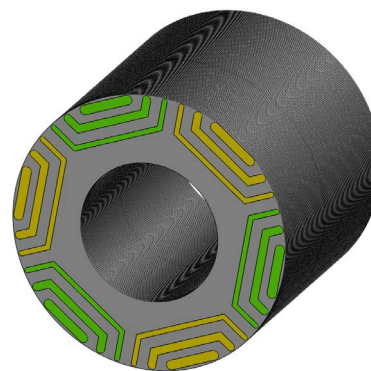

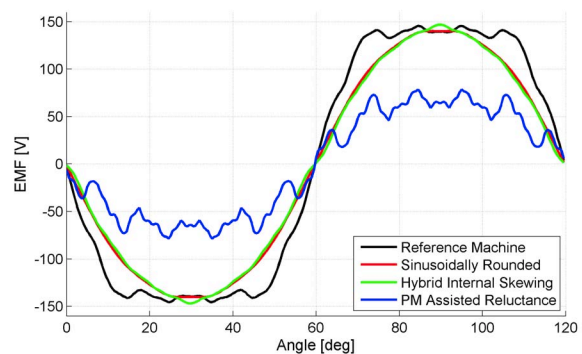Fig. 9. Assisted Reluctance Rotor
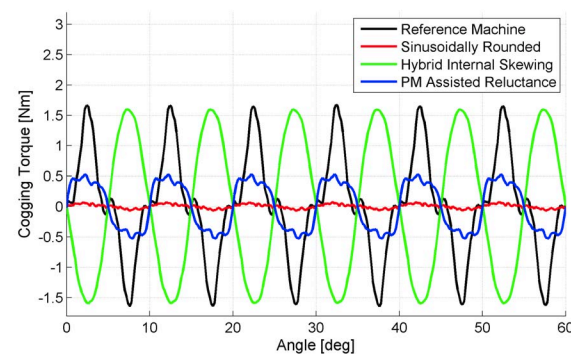

Fig. 10. Phase EMF Comparison

Fig. 11. Cogging Torque Comparison

The reduction of the production costs is evaluated based on the amount of magnetic material and taking into account that more complex geometries (rounded magnets and assisted reluctance) have higher cost for the same volume of magnetic material (Tab. IV). The comparison must be assessed in relation to the total cost of mass production of the machine, that is currently estimated in 190 dollars for the size taken into consideration.

To make a complete comparison also internal power factor is reported to consider the impact of the machine on the required drive size and therefore the overall cost of the application.

TABLE II
MAXIMUM STATOR FLUX DENSITY @ J = 4.5 A/MM^2

	Reference	Sinusoidally Rounded	Hybrid Internal Skewing	Reluctance	Assisted Reluctance	Units
Stator yoke	1.85	1.59	1.57	1.35	1.61	T
Stator teeth	1.80	1.74	1.77	1.65	1.80	T

TABLE III
COMPARISON OF THE DIFFERENT PERFORMANCE

	Reference	Sinusoidally Rounded	Hybrid Internal Skewing	Reluctance	Assisted Reluctance	Units
EMF$_{(a)}$ @ 1000rpm	120.4	104.2	103.6	-	53.9	$V_{(rms)}$
Cogging Torque	3.3	0.1	3.2	-	1.1	Nm
Internal Power Factor	0.995	0.990	0.989	0.652	0.921	-
Nominal Torque (@ j=4.5 A/mm^2)	32.0	28.2	28.0	16.0	24.2	Nm
Nominal Torque P.U.%	Reference	88%	88%	50%	76%	%
Torque Ripple	6.2	0.6	3.9	5.9	6.1	Nm
Torque Ripple P.U.%	Reference	9%	63%	95%	98%	%
Overload Torque (@ j=9 A/mm^2)	63.3	56.0	55.6	39.8	53.7	Nm
Overload Torque P.U.%	Reference	88%	88%	63%	85%	%
Overload Torque Ripple	10.8	1.3	4.8	19.9	9.8	Nm
Overload Torque Ripple P.U.%	Reference	12%	44%	185%	91%	%

TABLE IV
COMPARISON OF THE DIFFERENT ESTIMATED PM COSTS

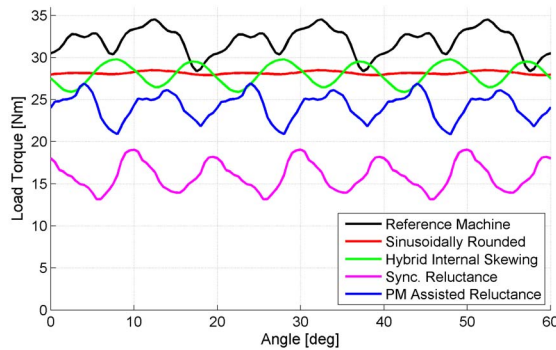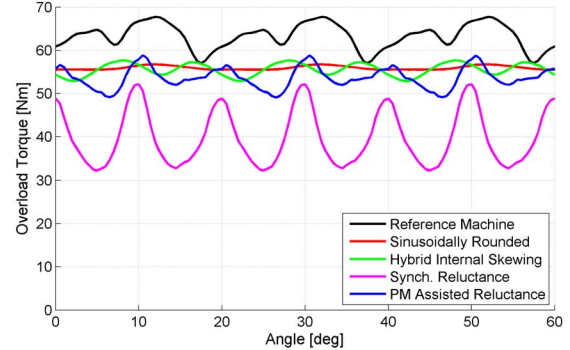|	Reference	Sinusoidally Rounded	Hybrid Internal Skewing	Reluctance	Assisted Reluctance	Units
NdFeB Volume	0.1677	0.1291	0.1009	-	-	dm^3
NdFeB Volume P.U.%	Reference	77%	60%	-	-	%
NdFeB Estimated Cost	59	56	36	-	-	$
Ferrite Volume	-	-	0.0668	-	0.2577	dm^3
Ferrite Estimated Cost	-	-	2	-	14	$
Machine PM Estimated Cost	59	56	39	0	14	$

Fig. 12. Nominal Torque Comparison

Fig. 13. Overload Torque Comparison

The Back-EMF of the hybrid and rounded solutions are nearly pure sine wave, while the reference machine back-EMF is more like a brushless DC machine wave form.

In [4] hybrid rotor reaches a cogging torque reduction of about 68%, while here its amplitude remain almost the same while its harmonics content is reduced.

This behavior is likely caused by:
- the teeth saturation of the commercial asynchronous stator
- the poor discretization of the ideal sinusoidal flux density distribution which is obtained by means of only two rotor steps. Nevertheless, the cogging torque is almost the 5.7% of the nominal torque and therefore the two step rotor solution could be the best trade-off between the quality of the machine

and the production costs. Instead, the optimized assisted reluctance rotor presents low cogging torque.

Using the rotor with hybrid PM, load torque ripple is greatly reduced both at nominal and overload conditions. It should be noted that torque ripple of the hybrid motor is mainly due to the cogging torque. Subtracting analytically this contribute, torque ripple result almost zero.

The pure reluctance motor presents lower mean-torque and higher torque-ripple than others solutions, but it is also the cheapest motor and there is no cogging torque. Nevertheless it must be considered that for the same electrical active power, this motor requires a drive of a grater size, because of its lower power factor value, that increases significantly the costs of the

system application. On the other hand this machine is capable of sensor-less control at very low speed and flux weakening operation.

The ferrite assisted reluctance machine has a nominal torque value close to the one of the surface permanent magnet solutions, also the power factor is improved compared to the pure reluctance solution. These results and the absence of the high cost NeFeB magnet could make this solution the best suited for many high efficiency applications.

VIII. CONCLUSIONS

The present work presents a comparison of different constructive solutions for low cost synchronous machine based on a readily available asynchronous stator frame.

The main design limitation lies into the induction machine stator, that is not optimized for PMSM and causes iron saturation and thus cogging torque and torque ripple.

The solution with sinusoidally profiled PM is the closest to the ideal AC brushelss machine, with the smallest torque ripple (only 9% of the reference machine) and almost no cogging torque, but it results to be the most expensive to manufacture. By discretizing the ideal sinusoidal flux density distribution using the proper combination of NdFeB and Ferrite magnets, the nominal mean torque remains high, the torque ripple is reduced to almost 37% of the reference machine and the use of NdFeB material is reduced by about 40%. In this case, the cogging torque hasn't reached a significant reduction as explained in the previous section, but as shown in [4] this method generally reduces cogging torque too. Therefore the Hybrid Internal skewing solution can be regarded a valid alternative to reduce the production costs while maintaining good performance. Ferrite assisted reluctance rotor presents a reduced cogging torque (33% of the reference machine), but the nominal torque is smaller (only 76% of the reference machine) and presents the greatest torque ripple (almost the same of the reference machine): different configurations of slot, pole and layer should be adopted in order to improve this topology of machine. The reduced cost of this topology of machine is in part compensated by the increased drive cost, due to inherent lower power factor. On the other hand this motor is capable of low speed sensor-less control and flux weakening operation.

REFERENCES

[1] "Efficiency classes of single-speed, three-phase, cage-induction motors (ie-code), ed. 1, iec 60034-30," *Rotating Electrical MachinesPart 30*, Nov 2008.

[2] "Efficiency classes of single-speed, three-phase, cage-induction motors (ie-code), ed. 1, iec 60034-2," *Rotating Electrical MachinesPart 30*, Sep 2014.

[3] A. Isfahani, S. Vaez-Zadeh, and M. Azizur Rahman, "Using modular poles for shape optimization of flux density distribution in permanent-magnet machines," *Magnetics, IEEE Transactions on*, vol. 44, no. 8, pp. 2009–2015, Aug 2008.

[4] C. Bianchini, M. Davoli, F. Immovilli, and E. Lorenzani, "Design optimization for torque ripple minimization and poles cost reduction with hybrid permanent magnets," pp. 483–489, Oct 2014.

[5] A. Vagati, M. Pastorelli, G. Francheschini, and S. Petrache, "Design of low-torque-ripple synchronous reluctance motors," *Industry Applications, IEEE Transactions on*, vol. 34, no. 4, pp. 758–765, Jul 1998.

[6] A. Boglietti and M. Pastorelli, "Induction and synchronous reluctance motors comparison," in *Industrial Electronics, 2008. IECON 2008. 34th Annual Conference of IEEE*, Nov 2008, pp. 2041–2044.

[7] G. Pellegrino, F. Cupertino, and C. Gerada, "Automatic design of synchronous reluctance motors focusing on barrier shape optimization," *Industry Applications, IEEE Transactions on*, vol. 51, no. 2, pp. 1465–1474, March 2015.